IEICE TRANSACTIONS

on Information and Systems

This advance publication article will be replaced by the finalized version after proofreading.

Evaluation of Multi-valued Data Transmission in Two-Dimensional Symbol Mapping using Linear Mixture Model*

Yosuke IIJIMA†, *Member*, Atsunori OKADA†, *Nonmember*, and Yasushi YUMINAKA††, *Senior Member*

SUMMARY   In high-speed data communication systems, it is important to evaluate the quality of the transmitted signal at the receiver. At a high-speed data rate, the transmission line characteristics act as a high-frequency attenuator and contribute to the intersymbol interference (ISI) at the receiver. To evaluate ISI conditions, eye diagrams are widely used to analyze signal quality and visualize the ISI effect as an eye-opening rate. Various types of on-chip eye-opening monitors (EOM) have been proposed to adjust waveform-shaping circuits. However, the eye diagram evaluation of multi-valued signaling becomes more difficult than that of binary transmission because of the complicated signal transition patterns. Moreover, in severe ISI situations where the eye is completely closed, eye diagram evaluation does not work well. This paper presents a novel evaluation method using Two-dimensional(2D) symbol mapping and a linear mixture model (LMM) for multi-valued data transmission. In our proposed method, ISI evaluation can be realized by 2D symbol mapping, and an efficient quantitative analysis can be realized using the LMM. An experimental demonstration of four leveled pulse amplitude modulation(PAM-4) data transmission using a Cat5e cable 100 m is presented. The experimental results show that the proposed method can extract features of the ISI effect even though the eye is completely closed in the server condition.
key words: *Multi-valued signaling, Intersymbol interference, Eye-opening monitor, Two-dimensional symbol mapping, Linear mixture model*

1. Introduction

Recently, multi-valued data transmission has been practically applied to serial-link systems in various fields such as high-capacity data center communications, further expanding its range of applications [1]. In paticular, the application of the four leveled pulse amplitude modulation (PAM-4) data transmission method, which replaces the conventional binary transmission method, is being actively considered. As shown in Fig. 1, at the same transmission rate, the symbol cycle of PAM-4 data transmission is $2\Delta t_{s-s}$ compared to the symbol cycle of binary transmission, Δt_{s-s}. In contrast, the symbol spacing is $\Delta V_{s-s}/3$ for PAM-4 transmission compared to ΔV_{s-s} for binary transmission. Because the Nyquist frequency can be reduced to half that of binary transmission by applying PAM-4 data transmission, the effect of intersymbol interference(ISI) caused by high-frequency attenuation in transmission lines can be reduced.

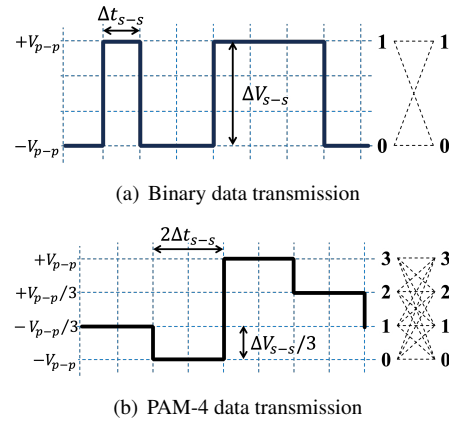Generally, to evaluate the signal quality, eye diagrams

(a) Binary data transmission

(b) PAM-4 data transmission

Fig. 1   Characteristics of signals and symbol transition patterns of binary and PAM-4 data transmission.

are used in high-speed data transmission, and the ISI can be visually represented using eye diagrams. Eye diagrams are generated by superimposing the received waveforms, and the signal quality can be evaluated using the aperture ratio of the width and height of the eye. As shown in Fig. 1(a), the symbol transition patterns in binary transmission are **0-1** and **1-0**; hence, the eye opens symmetrically at the center. However, in PAM-4 transmission, there are 16 symbol transition patterns, as shown in Fig. 1(b); therefore, the effect of the ISI is more complicated than in binary transmission, and the eyes have an asymmetric shape. As shown in Fig. 1(b), owing to the characteristics of the complicated symbol transition pattern in PAM-4, the shape of the eye between symbols **0-1** and symbols **2-3** becomes asymmetric. Therefore, the analysis of eye patterns in multi-valued data transmission should consider these characteristics. However, with the increasing severity of ISI, it is difficult to evaluate the eye pattern when the eye is completely closed.

To exclude ISI effects and achieve high-speed transmission, it is important to apply waveform shaping techniques such as FFE and DFE [2], [3]. On-chip eye-opening monitors (EOM), which are based on eye diagram evaluation, have been proposed to adjust the waveform shaping circuits [4]–[7]. Instead of evaluation based on eye diagram, an evaluation methodology using 2D symbol mapping, which visualizes the relationship between symbols, was proposed to visualize the signal quality for multi-valued data transmission[8]–[10]. ISI features can be extracted from a multi-domain map by plotting the received signals, and the

†The author is with the National Institute of Technology (KOSEN), Oyama College, JAPAN
††The author is with the Graduate School of Science and Technology, Gunma University, JAPAN

ISI effect can be analyzed in an eye diagram even when the eye is completely closed [11]. However, while 2D symbol map can visualize the ISI effect, quantitative numerical evaluation from 2D maps is essential.

This study presents a novel evaluation technique for analyzing the ISI effect on multi-valued data transmission using a 2D symbol map and a linear mixture model (LMM). By applying the LMM to represent the feature of the distribution of received signals on a 2D symbol map[12], the ISI effect on PAM-4 data transmission can be evaluated effectively compared with eye diagram evaluation in severe ISI conditions. This paper evaluates the effectiveness of transmission evaluation using 2D symbol maps and LMM in PAM-4 transmission, which is severely affected by ISI using LAN cables as the transmission line. In addition, we present symbol determination based on the results of LMM representation, and an experimental evaluation of this method and its validation results are discussed.

Section 2 explains the evaluation methodology using 2D symbol mapping, and Section 3 describes the evaluation techniques using and symbol determination using the LMM. Section 4 presents the experimental results and Section 5 discusses them. Finally, section 6 concludes the study.

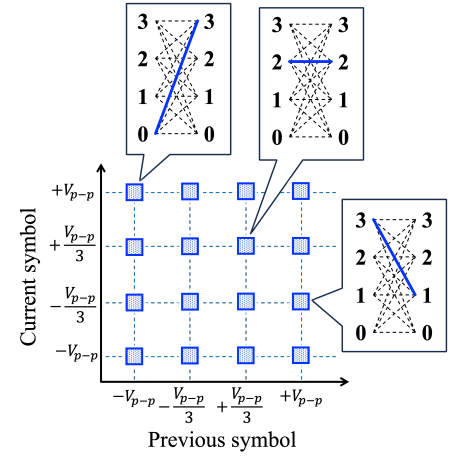## 2. ISI evaluation using 2D symbol mapping

In the PAM-4 data transmission, the ISI effect depends on a 16-symbol transition pattern, as shown in Fig. 1(b). Using 2D symbol mapping, the ISI effect, depending on the previous symbols, can be displayed to evaluate signal quality.

Figure 2 shows an overview of the evaluation using a 2D symbol map of the PAM-4 data transmission. To evaluate on the 2D symbol map, symbols of the PAM-4 signal were plotted on a 2D plane, in which the X- and Y-axes depict the received signal level of previous symbol values, x_{i-1}, and the received signal level of current symbol values, x_i, respectively. Plot (x_{i-1}, x_i) shows the relationship of received signals between the previous and next transmitted symbols as shown in Fig. 2(a). As shown in Fig. 2(b), if symbols **0**, **1**, **2**, and **3** are transmitted with signal levels $-V_{p-p}$, $-V_{p-p}/3$, $+V_{p-p}/3$, and $+V_{p-p}$, respectively, the PAM-4 received signals without ISI and attenuation effects are plotted as a 16-point grid pattern in the 2D symbol map. Each plot represents the relationship between the received signals for each symbol transition pattern.

However, under the influence of ISI, the distribution of the plots changed, as shown in Fig. 3. In the case of fewer ISI effects, the distribution of each symbol transition pattern widens, as shown in Fig. 3(a). The ISI widened the distribution of the plot clusters for each symbol transition pattern, causing an overlap in each cluster. Furthermore, as the effect of ISI worsened, the distribution of each plot cluster on the 2D map became skewed. The effect of the ISI can be evaluated from the slope of the plot distribution on the 2D symbol map. As shown in Fig. 3(a), if there is a space between the symbol distributions in the Y-axis direction, the eye is opened on the eye diagram. However,
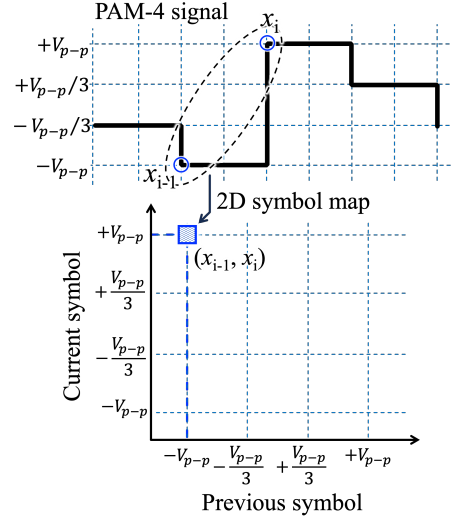
(a) 2D symbol map of PAM-4 without an ISI

(b) 2D symbol map of PAM-4 with an ISI

Fig. 2   Evaluation of symbol distribution using 2D symbol mapping.

(a) Fewer ISI effects   (b) Severe ISI effects
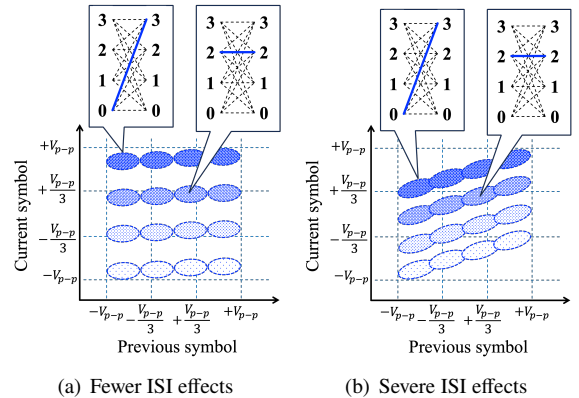
Fig. 3   Approximation of symbol distributions using linear mixture model.

if there is no space between the symbol distributions on the Y-axis direction, the eye is completely closed, as shown in
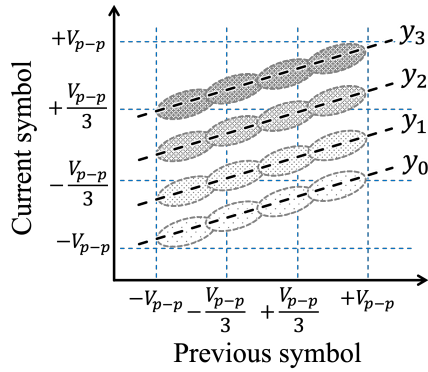
IIJIMA et al.: EVALUATION OF MULTI-VALUED DATA TRANSMISSION IN TWO-DIMENSIONAL SYMBOL MAPPING USING LINEAR MIXTURE MODEL

3

Fig. 4 Evaluation of a symbol overlap using the linear mixture model result.

Fig. 5 Calculation method of the variable error δ_{error}.

Fig. 3(b).

3. ISI evaluation using Linear Mixture Model

3.1 Distribution model using Linear Mixture Model for PAM-4 on 2D symbol map

The LMM was introduced to quantify the distribution of the received signals plotted on a 2D symbol map. As explained in Section 2, the plot of the received signal of PAM-4 on the 2D symbol map changes owing to ISI, resulting in a distribution with a slope for each symbol. In this study, the LMM quantifies the characteristics of each of the four transmitted symbols on a 2D symbol map.

$$\begin{bmatrix} y_0(x_{i-1}) \\ y_1(x_{i-1}) \\ y_2(x_{i-1}) \\ y_3(x_{i-1}) \end{bmatrix} = b_0 x_{i-1} + \begin{bmatrix} \mu_0 \\ \mu_1 \\ \mu_2 \\ \mu_3 \end{bmatrix}, \qquad (1)$$

where b_0 and μ_i are the slope and intercept, respectively. x_{i-1} represents the received signal level of previous symbols. Subsequently, y_0 to y_3 shows the distribution for each of the four PAM-4 symbols, and $y_0(x_{i-1})$ to $y_3(x_{i-1})$ shows the estimated received signal x_i for each symbol when the previous symbol is x_{i-1}. b_0 represents the slope of the line, and Eq. (1) models the slope of the four lines as the same. Figure 4 shows the approximation of the distributions of the plots on 2D symbol map using the LMM. As shown in Fig. 4, using the LMM, the features of relationship of the PAM-4 received signal can be expressed. The ISI effect can be evaluated by b_0 of LMM. The slope b_o becomes zero without the ISI effect. If the ISI effect increases, the slope of the distribution on the 2D symbol map increases, thus increasing b_0. The difference between each μ_i corresponds to the symbol spacing. By comparing the values of μ_i, we can check the uniformity of the distance between symbols and verify the non-linearity of the transmission level.
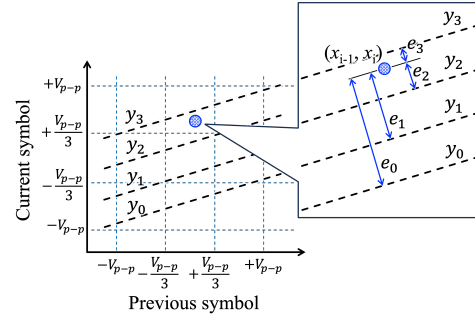
3.2 Parameter adjustment for LMM

To parameterize the LMM from the results of the plot on 2D symbol map, the following variable error δ_{error} is minimized:

$$\delta_{error} = \sum_{i=0}^{n} e_i = \sum_{i=0}^{n} \min_j \frac{|b_0 x_{i-1} - x_i + \mu_j|}{\sqrt{b_0^2 + 1}}, \qquad (2)$$

where x_i and x_{i-1} denote signal levels both the current and the previously received signals, respectively. In Eq. (2), the distance between a point (x_{i-1}, x_i) and each line $y_j = b_0 x_{i-1} + \mu_j$ is calculated. Then, the distance between the point (x_{i-1}, x_i) and the nearest line is selected, and the distance set as e_i. The δ_{error} is calculated as the sum of this e_i for n number of plots on the 2D symbol map. To obtain the LMM that can represent the distribution of the plots on a 2D symbol map, the parameters are optimized that minimized the error function δ_{error}.

Figure 5 shows an example of the calculation of the e_i between the received signal and LMM lines. These four lines show the y_0, y_1, y_2, and y_3, which were calculated using the LMM. As shown in Fig. 5, the errors(e_0, e_1, e_2, e_3) between the point (x_{i-1}, x_i) and the LMM lines were calculated, and the nearest line was selected. For example, e_0 is calculated by

$$e_0 = \frac{|b_0 x_{i-1} - x_i + \mu_0|}{\sqrt{b_0^2 + 1}}, \qquad (3)$$

and the smallest e_3 can be e_i as shown in Fig. 5. Similarly, we calculated the minimum distance of plots (x_{i-1}, x_i) for each received signal. The LMM parameters (b_0 and μ_i) were adjusted by searching for the parameter that minimized the sum of the errors, as shown in Eq. (2).
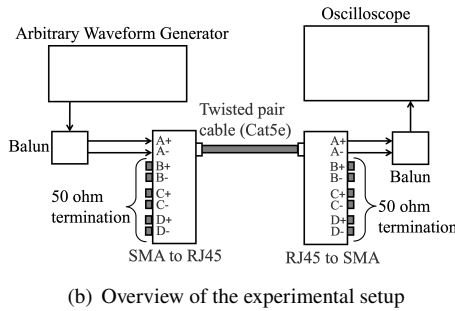
4. Experimental evaluation of PAM-4 using the LMM

4.1 Experimental setup of PAM-4 data transmission on Cat5e cable

In this study, to investigate transmission distortion in PAM-4, a PAM-4 transmission evaluation system was constructed
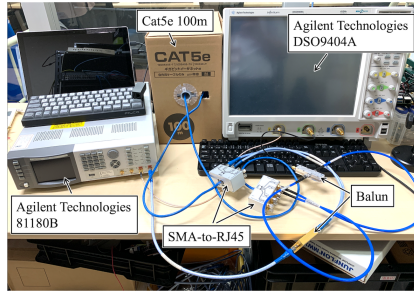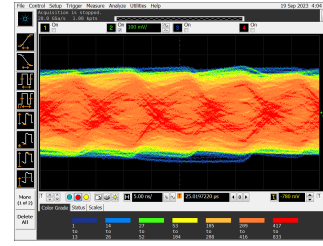
(a) Experimental setup

(b) Overview of the experimental setup

Fig. 6 Experimental setup using Cat5e cable.

(a) Measurement result of eye diagram

(b) 2D symbol mapping

(c) Distribution of samples for each symbol transition pattern

Fig. 7 Evaluation result of 2D symbol mapping using the experimental result of the received symbol at 200 Mbps PAM-4 on Cat5e 100 m.
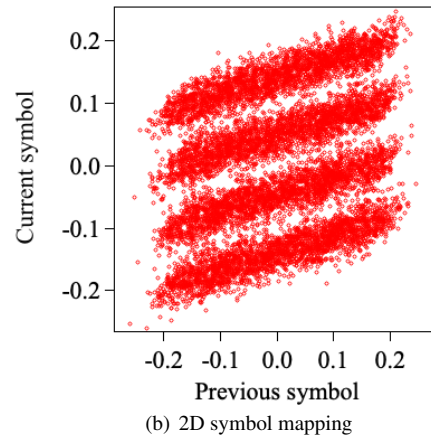
using LAN cables. A overview of the experiment system is presented in Fig. 6. As shown in the Fig. 6, an arbitrary waveform generator(Agilent Technologies 81180B) was used to generate PAM-4 waveforms, and the transmission distortion was observed on a LAN cable with an oscilloscope(Agilent Technologies DSO9404A). The outputs of the arbitrary waveform generator and the LAN cable are connected through a balun. The balun converted an unbalanced circuit signal from an arbitrary waveform generator into a balanced circuit signal and connected it to a LAN cable. The LAN cable is connected using an SMA-to-RJ45 converter. In this experiment, only one pair of twisted pair cables was used for each of the four twisted pair LAN cables, while the others were 50 Ω terminated. In the experiment, only one pair of twisted pair cables was used for each of the four twisted pair LAN cables, while the others were 50 Ω terminated. Figure 6(a) shows an overview of the experimental setup. As shown in Fig. 6(b), a 100 m Cat5e (SANWA SUPPLY Co. Ltd, 500-LAN5-CB100BL) cable was used as the LAN cable, which provides sufficient attenuation for the frequencies output by the arbitrary waveform generator. The transmission loss between the arbitrary waveform generator and oscilloscope was −21.654, −27.827, and −35.975 dB at 50, 100, and 200 MHz, respectively.
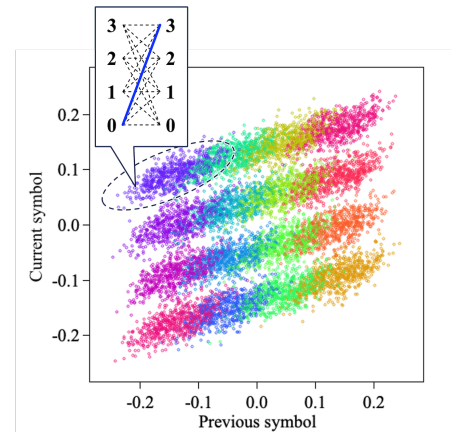
4.2 LMM evaluation of PAM-4 data transmission

Figure 7 shows the experimental results of the eye pattern and 10000 samples of data on a 2D symbol map at a transmission rate of 200 Mbps on a 100 m Cat5e cable. As shown in Fig. 7(a), the eye pattern is completely closed because of the ISI effect, and it is difficult to evaluate the eye height and eye width. Figure 7(b) shows a plot of the received waveform samples on the 2D symbol map. The received waveform data were oversampled using an oscilloscope, and using these data, the received symbols were sampled at each symbol interval. To verify the effectiveness of the evaluation method based on the 2D symbol map, the sampling timing was manually adjusted. As shown in Fig. 7(b), the features of the received sample that cannot be confirmed by the eye pattern can be seen on the 2D symbol map. Figure 7(c) shows the distribution of the received samples for each symbol transition pattern. As shown in Fig. 7(c), it can be seen on the 2D symbol map how the symbol distribution of the 16 patterns in PAM-4 is dispersed due to the effect of ISI.
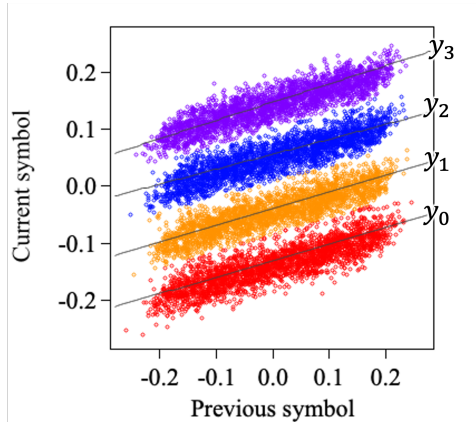
IIJIMA et al.: EVALUATION OF MULTI-VALUED DATA TRANSMISSION IN TWO-DIMENSIONAL SYMBOL MAPPING USING LINEAR MIXTURE MODEL

5

Fig. 8 Result of linear mixture model evaluation on 2D symbol map at 200 Mbps PAM-4 on Cat5e 100 m.

Table 1 Fitting parameters of linear mixture model

Parameter	200 Mbps(Fig. 8)	400 Mbps (Fig. 9)
b_0	0.328203	0.717205
μ_0	-0.135583	-0.073591
μ_1	-0.046191	-0.025722
μ_2	0.045538	0.024346
μ_3	0.135393	0.071972

Figure 8 shows the experimental results of the LMM evaluation. The 2D plot results are displayed in four different colors for each transmission symbol in Fig. 8. Both b_0 and μ_i, which are parameters of the LMM, were adjusted using the steepest descent method. The steepest descent method is used to search for the parameter that minimizes the error of Eq.(2). In parameter optimization, the initial value of b_0 is set to zero. The initial value of the intercept is set from the mean a and variance S of the sampled values of the received signal as $\mu_0 = a - 1.5S$, $\mu_1 = a - 0.8S$, $\mu_2 = a + 0.8S$ and $\mu_3 = a + 1.5S$. In the result of parameter adjustment of Fig. 8, b_0, μ_0, μ_1, μ_2 and μ_3 are presented as Table 1.

Figure 9 shows the experimental results at 400 Mbps PAM-4 on the 100 m Cat5e cables. As shown in Fig. 9(a), the eye was completely closed owing to the ISI effect, and the significant overlap between the symbols increased, as shown in Fig. 9(b). The increased ISI complicates recognition on a 2D symbol map: despite this issue, the LMM can extract symbol distribution features when the symbols do not fully overlap, as shown in Fig. 9(c). The parameters of the LMM are listed in Table 1. Analysis was conducted using real numbers, as shown in Table 1. The significant digits in LMM analysis needed to be selected based on the resolution of the analog-to-digital converter (ADC) in the received signal.

4.3 Symbol determination using result of LMM

The LMM shows the distribution of sampling values for each transmitted symbol at the receiver. Using the LMM results, symbol determination of an unknown received signal is possible. Figure 10 shows an overview of symbol determination by using LMM. As shown in the Fig. 10(a), we first plot a cer-
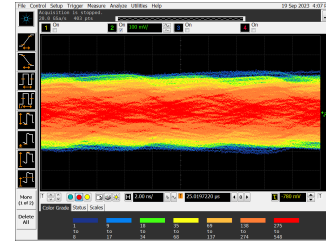
(a) Measurement result of eye diagram
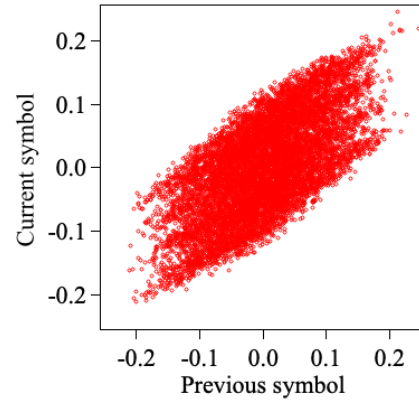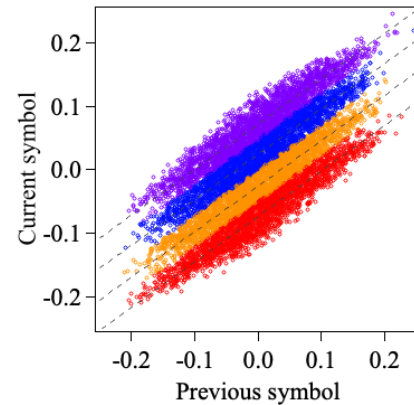
(b) 2D symbol mapping


(c) Result of linear mixture model evaluation on 2D map

Fig. 9 Evaluation result of 2D symbol mapping using experimental result of received symbol at 400 Mbps PAM-4 on Cat5e 100 m.

tain number of sampled values at the receiver on a 2D symbol map. Then, LMM parameters are obtained as described in Section 4.2. Using the LMM, symbol determination is performed based on the minimum value of each linear distance between the point and LMM lines on the 2D symbol map for unknown sampling symbols, as shown in Fig. 10(b).

Figure 11 depicts the experimental results of the PAM-4 symbol classification at 200 Mbps on the 100 m cat5e cable. Figure 11(a) shows the received waveform. The LMM parameters were determined using the first 100 samples in the received waveform. The symbols of the sampled values in the second half were then determined using the determined LMM. Figure 11(b) shows a 2D symbol map of 100 sam-
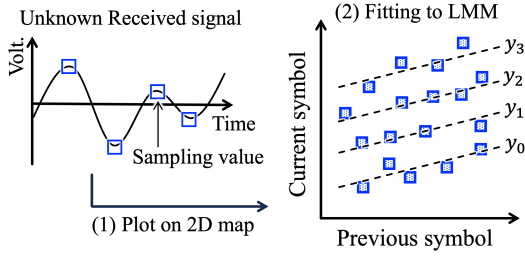
(a) How to obtain the LMM lines
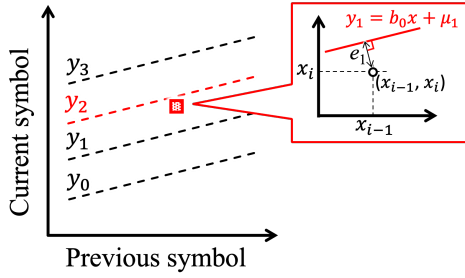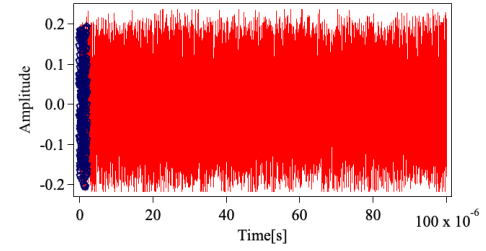

(b) Symbol classification method

Fig. 10 Overview Symbol classification using linear mixture model.

(a) Received waveform (○ is sampling values for LMM fitting)

(b) Result of linear mixture model evaluation using 100 samples

(c) Result of symbol classification

Fig. 11 Symbol classification using linear mixture model at 200 MHz PAM-4.

ples in the first half of the received waveform. Four straight lines of the LMM determined from these 100 samples were overlaid on a 2D symbol map. Figure 11(c) shows the results of symbol determination using the LMM results for an unknown received signal. In Fig. 11(c), the symbol classification results are displayed in different colors. Correctly classified symbols are denoted by blue circles, and inconsistent classifications are represented by red circles. As shown in Fig. 11(c), for an unknown received signal plotted on the 2D symbol map, the symbol can be determined almost correctly by calculating the distance to the straight line of the LMM, which is obtained using the 100 samples, and judging it as the symbol of a nearby straight line.

5. Discussion

The results in the Fig. 7 show that the 2D symbol map and LMM can visualize and effectively quantify the effects of the ISI, which are difficult to evaluate using eye patterns. A histogram of the sampled values of the received waveforms for the same results is shown in Fig. 12. With eyes closed, the received signals are a single population on the histogram, as shown in Fig. 12(a). Figure 12(b) shows a histogram of the received signal for each transmitted symbol, separated and color-coded. As shown in the Fig. 12(b), when the eye was closed, the histogram distribution of each symbol overlapped. Although it is possible to numerically analyze and visualize it using a Gaussian mixture model from the histogram of an unknown received signal [13], [14], direct observation of the ISI effect from the histogram is difficult. Furthermore, an evaluation using histograms requires sufficient number of samplings for statistical analysis.
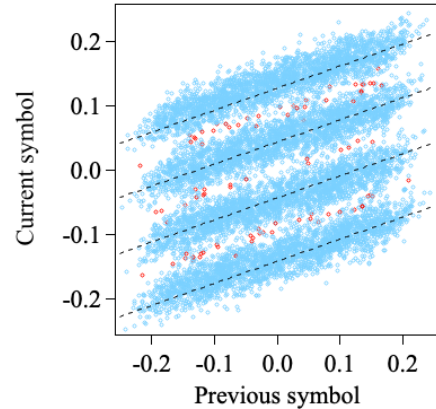
Figure 13 shows the results of the evaluation using
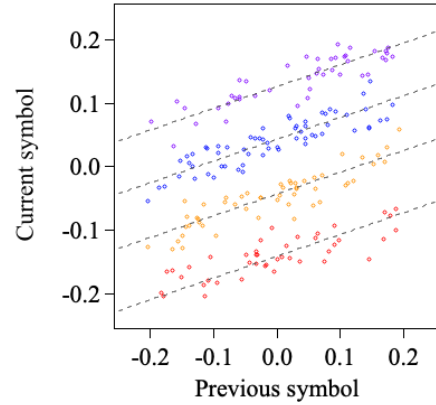
the LMM for different sampling numbers. The LMM fitting results for the 50, 100, and 200 samples are shown in Figs. 13(b), 13(c), and 13(d), respectively. In the Fig.13, in addition to the 2D symbol map results, histograms of the received signal for each transmitted symbol and the histogram of the entire received signal are shown. As shown in Fig. 13(b), regardless of the small number of samples, LMM can extract the features of the received signal. It can be observed that histograms with the same number of samples are difficult was considered statistically significant. As shown in Figs. 13(c), and (d), by increasing the number of samples, the LMM can more accurately represent the characteristics
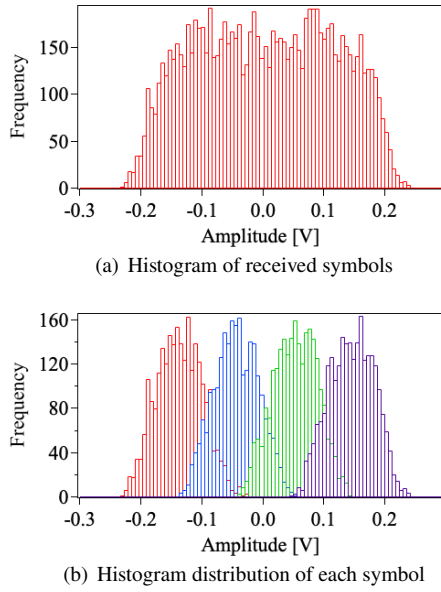
IIJIMA et al.: EVALUATION OF MULTI-VALUED DATA TRANSMISSION IN TWO-DIMENSIONAL SYMBOL MAPPING USING LINEAR MIXTURE MODEL

7

(a) Histogram of received symbols

(b) Histogram distribution of each symbol

Fig. 12 Histogram evaluation of received signal of result at 100 Mbps PAM-4 on Cat5e 100 m.

Table 2 Fitting parameters of LMM of each number of sampling

Parameter	50 samples	100 samples	200 samples	10000 samples
b_0	0.336393	0.315215	0.342820	0.328203
μ_0	-0.148436	−0.131260	-0.141016	-0.135583
μ_1	-0.044616	−0.042657	-0.042799	-0.046191
μ_2	0.028123	0.041814	0.043682	0.045538
μ_3	0.119981	0.121501	0.126955	0.135393

of the received signal. Table 2 presents the LMM parameters of each result of Fig. 13. The LMM parameters closely approximate the result obtained from 10000 samples, even with a small number of sampling result.

The relationship between the number of samples and the LMM fitting error is shown in Fig. 14. The horizontal axis of the Fig. 14 shows the number of samples used for the LMM fitting, and the vertical axis shows the symbol decision error in 10000 symbols using the LMM. In the Fig. 14, the dotted line represents each of the 10 evaluations, and the solid line represents the average. As shown in the Fig. 14, the number of errors decreases as the number of samplings increases, and it almost converges after approximately 200 samplings. This result indicates that the LMM on the 2D symbol map can be used to efficiently extract the effect of the ISI in PAM-4 transmission from a small number of samples. In this study, the LMM parameters were determined from the received signal at randomly transmitted symbols, without the use of known signals for LMM determination.

6. Conclusion

This paper proposes an evaluation method for signal integrity using a 2D symbol mapping with an LMM for multi-valued data transmission. The LMM can express the features of
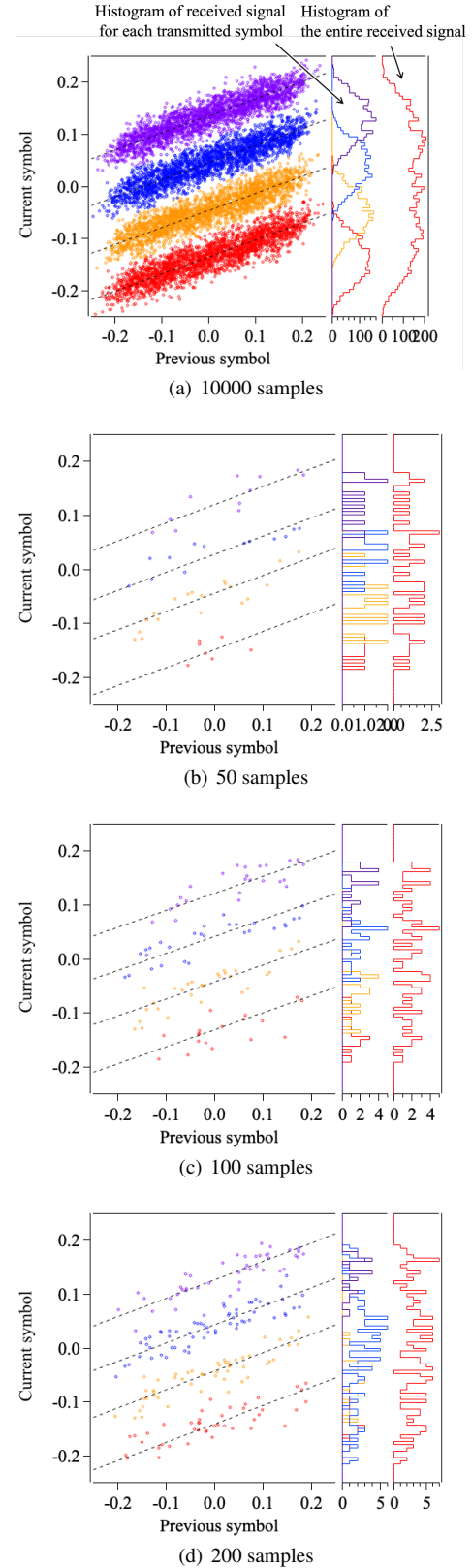

(a) 10000 samples

(b) 50 samples

(c) 100 samples

(d) 200 samples

Fig. 13 Comparison results of different number of sampling for LMM parameter fitting at 200 Mbps PAM-4 on Cat5e 100 m.
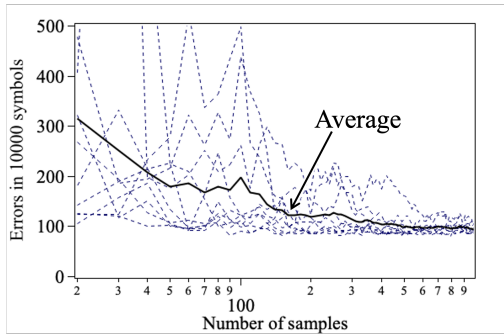
8

Fig. 14 Fitting error transitions for different sampling numbers at 200 Mbps PAM-4 on Cat5e 100 m.

the received signal of PAM-4 and quantify the ISI effect. The simulation results demonstrated that the LMM can fit the symbol distribution of PAM-4 with a severe ISI. Classification of unknown received symbols using the LMM was demonstrated. Because the LMM can estimate symbol distribution with a small number of samples, it can be expected to determine symbols in response to changes in the communication environment. As future work, the proposed method can be used to further extend signal quality analysis in terms of bit error rate. By deriving the variance of the received signal from the relationship between the received sample values for each symbol and the LMM, statistical signal quality analysis can be considered.

Acknowledgment

References

[1] E. Depaoli et al., "A 64 Gb/s Low-Power Transceiver for Short-Reach PAM-4 Electrical Links in 28-nm FDSOI CMOS," in IEEE Journal of Solid-State Circuits, vol. 54, no. 1, pp. 6-17, Jan. 2019, doi: 10.1109/JSSC.2018.2873602.

[2] Z. Toprak-Deniz et al., "A 128-Gb/s 1.3-pJ/b PAM-4 Transmitter With Reconfigurable 3-Tap FFE in 14-nm CMOS," in IEEE Journal of Solid-State Circuits, vol. 55, no. 1, pp. 19-26, Jan. 2020, doi: 10.1109/JSSC.2019.2939081.

[3] J. Kim et al., "A 224-Gb/s DAC-Based PAM-4 Quarter-Rate Transmitter With 8-Tap FFE in 10-nm FinFET," in IEEE Journal of Solid-State Circuits, vol. 57, no. 1, pp. 6-20, Jan. 2022, doi: 10.1109/JSSC.2021.3108969.

[4] H. Won et al., "A 28-Gb/s Receiver With Self-contained Adaptive Equalization and Sampling Point Control Using Stochastic Sigma-Tracking Eye-Opening Monitor," in IEEE Transactions on Circuits and Systems I: Regular Papers, vol. 64, no. 3, pp. 664-674, March 2017, doi: 10.1109/TCSI.2016.2614349.

[5] A. R. AL-Taee et al., "New 2-D Eye-Opening Monitor for Gb/s Serial Links," in IEEE Transactions on Very Large Scale Integration (VLSI) Systems, vol. 22, no. 6, pp. 1209-1218, June 2014, doi: 10.1109/TVLSI.2013.2267805.

[6] L. Chang et al., "A 50Gb/s-PAM4 CDR with On-Chip Eye Opening Monitor for Reference-Level and Clock-Sampling Adaptation," 2018 Optical Fiber Communications Conference and Exposition (OFC), San Diego, CA, USA, 2018, pp. 1-3.

[7] Y. -C. Lin et al., "A 10-Gb/s Eye-Opening Monitor Circuit for Receiver Equalizer Adaptations in 65-nm CMOS," in IEEE Transactions on Very Large Scale Integration (VLSI) Systems, vol. 28, no. 1, pp. 23-34, Jan. 2020, doi: 10.1109/TVLSI.2019.2935305.

[8] F. Lu et al., "Integration of Multivariate Gaussian Mixture Model for Enhanced PAM-4 Decoding Employing Basis Expansion," *2018 Optical Fiber Communications Conference and Exposition (OFC)*, -p.1-3, 2018.

[9] L.Sun et al., "Intelligent 2-Dimensional Soft Decision Enabled by k-means Clustering for VCSEL-based 112-Gbps PAM-4 and PAM-8 Optical Interconnection," *Journal of Lightwave Technology*, vol.37, no.24, pp.6133-6146, 2019.

[10] L. Sun et al., "Distortion-Aware 2D Soft Decision for VCSEL-MMF Optical PAM Interconnection," *2020 Optical Fiber Communications Conference and Exhibition (OFC)*, pp.1-3, 2020.

[11] Y. Yuminaka et al., "PAM-4 Data Transmission Quality Evaluation Using Two- and Three-Dimensional Mapping of Received Symbols," *IEEE 53rd International Symposium on Multiple-Valued Logic*, pp.94-98, 2023.

[12] Y. Iijima et al., "Evaluation and Symbol Classification of Multi-Valued Signaling Using Two-Dimensional Symbol Mapping with Linear Mixture Model," *IEEE 53rd International Symposium on Multiple-Valued Logic*, pp.99-104, 2023.

[13] Y. Iijima et al., "PAM-4 Eye-Opening Monitoring Techniques using Gaussian Mixture Model," *IEEE 50th International Symposium on Multiple-Valued Logic*, pp.149-154, 2020.

[14] Y. Iijima et al., "PAM-4 Eye-Opening Monitor Technique Using Gaussian Mixture Model for Adaptive Equalization," *IEEE Transactions on Information & Systems*, vol.104-D, no.8, pp.1138-1145, 2021.
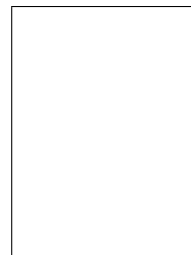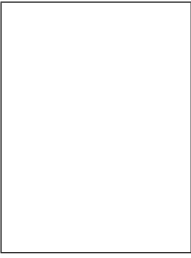
Yosuke Iijima received B. E. and M. E. degrees in electronic engineering from Gunma University, Kiryu, Japan, in 2003 and 2005, respectively, and received D. E. degree in electronic engineering from the University of Tsukuba, Japan, in 2008. He is currently an Associate Professor in the Department of Innovative Electrical and Electronic Engineering, National Institute of Technology (KOSEN), Oyama College, Oyama, Japan. His research interests include the design of high-speed interfaces, dig-sensor communication systems and their applications. Dr. Iijima received the Kenneth C. Smith Early Career Award in Microelectronics from the IEEE Computer Society Technical Committee on Multiple-Valued Logic in 2019. He served as a Program Co-Chair for IEEE International Symposium on Multiple-Valued Logic in 2023. He is a member of IEEE and IEEJ.
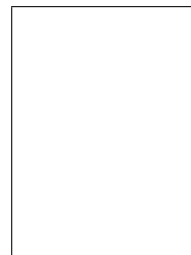
Atsunori Okada received A.E degree in electrical and electronic from National Institute of Technology, Oyama College, Japan, in 2023. He is currently a student of advanced engineering course of National Institute of Technology, Oyama College. His research interests include design of high-speed serial links using multi-valued logic.

IIJIMA et al.: EVALUATION OF MULTI-VALUED DATA TRANSMISSION IN TWO-DIMENSIONAL SYMBOL MAPPING USING LINEAR MIXTURE MODEL

9

Yasushi Yuminaka received B. E., M. E., and D. E. degrees in electronic engineering from Tohoku University, Sendai, Japan, in 1990, 1992, and 1995, respectively. He is currently a Professor in the Division of Electronics and Informatics, Graduate School of Science and Technology, Gunma University, Kiryu, Japan. His research interests include the design of multiple-valued integrated circuits, high-speed interfaces for VLSI systems, and new-paradigm computing systems and their applications. Dr. Yuminaka received the IEE Ambrose Fleming Premium Award in 1994, the Niwa Memorial Award in 1995, the Young Engineer Award from the IEICE of Japan in 1995, and the Outstanding Contributed Paper Award at the IEEE International Symposium on Multiple-Valued Logic in 2000 and 2009. He served as a Program Chair for IEEE International Symposium on Multiple-Valued Logic in 2013, 2016, and 2020, and a Symposium Chair for IEEE International Symposium on Multiple-Valued Logic in 2023. He was a Chair (2020-2021) of the IEEE Computer Society Technical Committee on Multiple-Valued Logic. He is senior members of IEEE and IEEJ